AFGL-TR-77-0262
ENVIRONMENTAL RESEARCH PAPERS, NO. 615

Thermal and Hyperthermal Electron Distributions in the Midnight Sector of the Winter Topside Ionosphere

W. J. BURKE
R. C. SAGALYN
M. KANAL

ADA051419

AD No.
DDC FILE COPY

D D C
MAR 20 1978
F

28 November 1977

This report has been reviewed by the ESD Information Office (OI) and is releasable to the National Technical Information Service (NTIS).

This technical report has been reviewed and is approved for publication.

FOR THE COMMANDER

Chief Scientist

SECURITY CLASSIFICATION OF THIS PAGE (When Data Entered)

(9) Environmental Research Papers

REPORT DOCUMENTATION PAGE	READ INSTRUCTIONS BEFORE COMPLETING FORM

1. REPORT NUMBER (14) AFGL-TR-77-0262, AFGL-ERP-615	2. GOVT ACCESSION NO.	3. RECIPIENT'S CATALOG NUMBER

4. TITLE (and Subtitle) (6) THERMAL AND HYPERTHERMAL ELECTRON DISTRIBUTIONS IN THE MIDNIGHT SECTOR OF THE WINTER TOPSIDE IONOSPHERE	5. TYPE OF REPORT & PERIOD COVERED Scientific. Interim.
	6. PERFORMING ORG. REPORT NUMBER ERP, No. 615

7. AUTHOR(s) (10) W. J. Burke, R. C. Sagalyn, M. Kanal**	8. CONTRACT OR GRANT NUMBER(s)

9. PERFORMING ORGANIZATION NAME AND ADDRESS Air Force Geophysics Laboratory (PHR) Hanscom AFB, Massachusetts 01731	10. PROGRAM ELEMENT, PROJECT, TASK AREA & WORK UNIT NUMBERS 61102F (14) 2311G205 (17)(G2)

11. CONTROLLING OFFICE NAME AND ADDRESS Air Force Geophysics Laboratory (PHR) Hanscom AFB, Massachusetts 01731	12. REPORT DATE (11) 28 November 1977
	13. NUMBER OF PAGES 27 (72) 28 P.

14. MONITORING AGENCY NAME & ADDRESS(if different from Controlling Office)	15. SECURITY CLASS. (of this report) Unclassified
	15a. DECLASSIFICATION/DOWNGRADING SCHEDULE

16. DISTRIBUTION STATEMENT (of this Report)

Approved for public release; distribution unlimited.

17. DISTRIBUTION STATEMENT (of the abstract entered in Block 20, if different from Report)

18. SUPPLEMENTARY NOTES

*Regis College Research Center, Weston, Massachusetts 02193

**University of Lowell, Center for Atmospheric Research, Lowell, Massachusetts 01854

19. KEY WORDS (Continue on reverse side if necessary and identify by block number)

Conjugate photoelectron heating
Mid-latitude electron temperatures

20. ABSTRACT (Continue on reverse side if necessary and identify by block number)

A gridded spherical electrostatic analyzer aboard Injun 5 has been used to measure fluxes of thermal and hyperthermal electrons at sub-auroral latitude in the midnight sector of the northern ionosphere between altitudes of 2500 and 850 km. Due to the offset between the geomagnetic and geographic poles, hyperthermal fluxes consisting of energetic photoelectrons that have escaped from the sunlit southern hemisphere are observed along orbits over the Atlantic Ocean and North America but not over Asia. The ambient electron temperatures near 2500 km have their highest values at trough latitudes for

DD FORM 1 JAN 73 1473 EDITION OF 1 NOV 65 IS OBSOLETE

Unclassified

SECURITY CLASSIFICATION OF THIS PAGE (When Data Entered)

20.   (Cont)

all longitudes. At altitudes near 1000 km, elevated electron temperatures in the trough were not a consistent feature of the data. Equatorward of the trough, electron temperature distributions are functions of longitude. In the longitude sector to which conjugate photoelectrons have access, T ~ 4000°K at 2500 km and ~ 8000°K at 1000 km. For regions with the conjugate point in darkness, T_e ~ 2300°K over the 1000 to 2500 km altitude range. Effective spectral characteristics of the photoelectrons are studied as functions of latitude and altitude. Based on these observations it is concluded that:

(1) At trough latitudes, elevated electron temperatures in the topside ionosphere are produced by sources other than conjugate photoelectrons,

(2) Equatorward of the trough in the Atlantic Ocean, North American longitude sector conjugate photoelectrons contribute significantly to the heating of electrons in the topside ionosphere. Much of the photoelectron energy is deposited at altitudes greater than 2500 km, then conducted along magnetic field lines into the ionosphere.

Contents

Illustrations

Thermal and Hyperthermal Electron Distributions in the Midnight Sector of the Winter Topside Ionosphere

1. INTRODUCTION

The possibility of significant heating of the nighttime ionosphere by energetic photoelectrons that have escaped from the sunlit conjugate ionosphere was first suggested by Hanson.[1] Several theoretical models for the production and transport of these electrons have been developed. Cicerone et al[2] and Swartz[3] have compared the escape fluxes of photoelectrons predicted by diffusion,[4,5] two-stream[6,7] radiative transfer,[8] and Monte Carlo[9,10] type models. Agreement, within a factor of two, was found. Similar calculations were also performed by Mantas and Bowhill[11] using an exact solution to the Boltzmann equation.[12] A theoretical analysis by Lejuene and Wormser[13] predicts that due to collisions within the protonosphere the escaping photoelectron flux is reduced by a factor of two before reaching the conjugate ionosphere. Heating[14] and possible ionization[15] effects of conjugate photoelectrons (CPE's) at altitudes < 600 km in the conjugate ionosphere have also been computed.

Measured fluxes of photoelectrons escaping from the sunlit ionosphere have been reported by a number of investigators.[16-22] The intensity of these fluxes is significantly reduced when they reach the conjugate ionosphere with the greatest degradation in the low energy portion of the spectrum.[18,20,22]

The heating effects of CPE's in the darkened ionosphere were first observed *in the form of enhanced predawn airglow.* [23] Observations of CPE produced radiative emissions were reviewed by Carlson. [24] Incoherent backscatter techniques have been used to detect significant ionospheric temperature increases over Arecibo at the time of conjugate sunrise. [25] Although radar signals showed that CPE's were reaching to the ionosphere over Millstone Hill, [26] much smaller temperature increases were detected in the 375 ± 40 km altitude range. [27] The predawn temperature differences were explained in terms of greater transmission losses along the Millstone Hill—conjugate point field line. Direct measurements of CPE produced temperature increases at altitude > 2000 km at low latitudes ($1.2 \leq L \leq 2.5$) were reported by Rao and Maier. [18] The ionization produced by conjugate photoelectrons has been found to be much less than was theoretically predicted by Shawhan et al[15] and Nagy et al. [28]

In this report we present observations of longitudinal and latitudinal distributions of thermal and hyperthermal electrons in the late-evening sector of the winter, topside ionosphere. Measurements were made by means of the spherical electrostatic analyzer (SEA) aboard the polar orbiting satellite Injun 5 near the times of the 1968 and 1969 winter solstices. In Section 2 we first describe the SEA and its modes of operation. For heuristic purposes, we calculate the latitudes and longitudes at which a satellite at an *altitude of 2000 km in the midnight sector is expected to* encounter CPE fluxes. In Section 3 we present Injun 5 observations from the North American and Asian longitudinal sectors. Hyperthermal electrons, shown to be CPE's are found at subauroral latitudes over North America but not over Asia. Spectral characteristics of CPE's are discussed briefly. The heating effects of CPE fluxes are studied by comparing electron temperature (T_e) between invariant latitudes (Λ) 70° and 40° in the altitude (h) range 2500 to 850 km observed over North *America and Asia. In Section 4 we assume that the ionospheric properties mea*sured by Injun 5 are representative of the mid-latitude, winter, topside ionosphere.

23. *Barbier, D. (1959) Recherches sur la raie 6300 de la luminescence atmos*pherique nocturne, Ann. Geophs. 15:179-186.

24. Carlson, H. C. (1974) Survey of satellite and ground based measurements of photoelectron excited emissions, Ann. Geophys. 30:59.

25. Carlson, H. (1966) Ionospheric heating by magnetic conjugate-point photoelectrons, J. Geophys. Res. 71:195.

26. Evans, J. V., and Gastman, I. J. (1970) Detection of conjugate photoelectrons at Millstone Hill, J. Geophys. Res. 75:807.

27. Evans, J. V. (1968) Sunrise behavior of the F layer at midlatitudes, J. Geophys. Res. 73:3489.

28. Nagy, A. F., Winningham, J. D., and Banks, P. A. (1973) The effect of conjugate photoelectron impact ionization on the pre-dawn ionosphere, J. Atm. Terr. Phys. 35:2289.

This allows us to construct a statistical model and to examine average thermal gradients along magnetic field lines. Some transport characteristics of the region are estimated.

Thermal gradients and CPE generated heat fluxes are found to be approximately a factor of three greater than those calculated by Rao and Maier.[18]

2. INSTRUMENT AND METHOD OF ANALYSIS

Injun 5 is a magnetically aligned polar orbiting satellite with an inclination of 81°, an apogee of 2543 km and a perigee of 677 km. The experiment discussed in this report is a spherical electrostatic analyzer mounted on a 5-ft boom. The instrument design and the modes of data reduction are described by Burke et al.[29] Briefly, the electron sensor consists of a solid tungsten collector of 0.5-in. radius surrounded by two tungsten wire mesh grids of 1-in. and 1.25-in. radii. The grids are electrically connected and are alternately swept from -10 to +3 V (Mode 2) for 15.9 sec then rest at either 1.6 or 6.2 V (Mode 1). The purpose of the grid bias is to counteract expected negative satellite potentials. The potential of the collecting sphere is held at +100 V. From data obtained in the Mode 1 and 2 sequence we generally are able to measure the electron density and temperature as well as the vehicle potential with respect to the plasma. In processing the data we follow procedures first outlined by Mott-Smith and Langmuir.[30]

During November/December 1968 and January 1970, Injun 5 was in the late evening-midnight sector. We can thus examine a large data segment over the northern (winter) ionosphere. Of particular interest are the thermal and hyperthermal electron fluxes observed between 70° and 40° invariant latitude. Because the satellite was near apogee during the 1968 period and between 1400 and 850 km during January 1970 we treat the data sets separately before comparing them. Also, to avoid confusing CPE and magnetic storm related heating effects, we have eliminated all storm-time data from consideration. Injun 5 storm-time observations are described in a separate study.[31]

The term "conjugate orbit" is useful for designating the satellite's trajectory mapped to an altitude of 300 km in the conjugate ionosphere. This altitude was chosen as the top of the production region in the sunlit ionosphere. It is assumed

29. Burke, W.J., Donatelli, D.E., and Sagalyn, R.C. (1978) Injun 5 observations of low energy plasma in the high latitude topside ionosphere, (to be published J. Geophys. Res.).

30. Mott-Smith, H.M., and Langmuir, I. (1926) The theory of collectors in gaseous discharges, Phys. Rev. 28:727-763.

31. Rao, L.V.D., Burke, W.J., Kanal, M., and Sagalyn, R.C. (1978) Injun 5 low energy plasma observations during a major magnetic storm, (to be published J. Geophys. Res.).

that any photoelectron reaching this altitude has a mean free path much longer than the ionospheric scale height and can be considered as having escaped. Aside from losses due to collisions with magnetospheric particles these photoelectrons travel freely along magnetic field lines to the opposite hemisphere. By calculating the solar zenith angle along the conjugate orbit we can determine when and where Injun 5 can be expected to encounter CPE's.

Near the time of the winter solstice, the southern hemisphere of the ionosphere is most exposed to solar radiation and CPE fluxes can be observed in the night-side, northern ionosphere. The latitudes at which these CPE fluxes are observed depends on the longitude of observations. This is due to the offset between the geographic and geomagnetic poles. When the south magnetic pole is near local noon, escaping photoelectrons have access to the night-side, northern ionosphere. This is not true when the south pole is near local midnight. This effect is illustrated in Figure 1 where we have plotted the contours of constant conjugate solar zenith angle for a given northern magnetic latitude as a function of geographic longitude at an altitude of 2000 km. The calculations were made assuming that: (1) the longitude in question was at local midnight in the northern hemisphere, (2) the time of year was the winter solstice, and (3) the south magnetic pole is at 75° S, 127° E. [32] The contours of Figure 1 indicate that the deepest low latitude penetration of CPE fluxes occurs between 60° and 90° W longitude, that is, from the middle of the Atlantic Ocean to central North America. Conversely, CPE fluxes are excluded from the Asian sector (60° to 120° E) at subauroral latitudes.
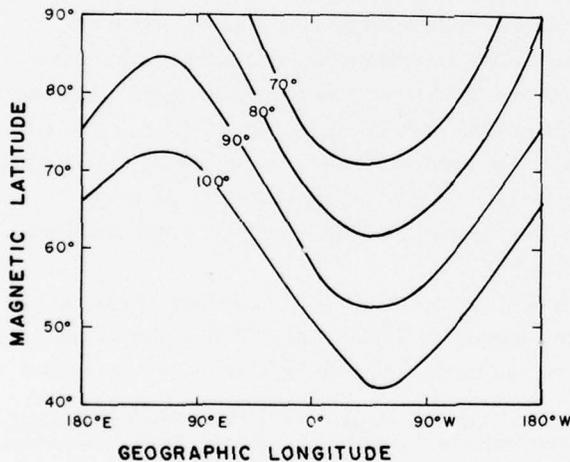
Figure 1. Contours of Constant Solar Zenith Angles at 300 km in the Conjugate Hemisphere for Different Northern Hemisphere Magnetic Latitudes as a Function of Geographic Longitude. Calculations were made for the midnight sector at the time of the winter solstice

32. Gustafson, G. (1970) A revised corrected geomagnetic coordinate system, Arkiv for Geofysik 5:595-617.

10

3. OBSERVATIONS

3.1 Basic Data

To illustrate quiet-time, winter observations at subauroral latitudes, in Figure 2 we have plotted the omnidirectional flux to the electron sensor during Injun 5 orbits #1331 and #1325 as functions of universal time (UT) and the McIlwain L parameters. Alternating high and low flux values result from the sensor's Mode 1 and Mode 2 electronic sequencing as identified at 0605 UT. The altitude, longitude and local time of the orbits given at L = 2 and 4 show that the satellite was near apogee in the late evening sector over the northern hemisphere. Orbit #1331 was over central North America and #1325 over western Siberia. That magnetic conditions were quiet is evidenced by auroral electrojet indices (AE) of 35 and 52.

In the region $6.5 \leq L \leq 3.7$ the Mode 2 sweeps of orbit #1331 are characterized by two positive slopes. This indicates the presence of a hyperthermal as well as a thermal electron population. Similarities between these and the data of Maier and Rao[17] suggests that CPE's constitute the hyperthermal population. For $L < 3.6$ the slope of the hyperthermal flux changes from positive to negative values. Current vs applied voltage curves recorded during the four Mode 2 sweeps of orbit #1331 marked A, B, C, and D are given in Figure 3. In all four cases the currents remain at relatively low levels for $V < -1$ volt. For $V > -1$ V the currents rise steeply as thermal electrons are allowed to reach the collector.

The decreasing electron currents with increasing applied grid voltages, found in the extreme retarding portion of sweeps C and D, result from secondary electrons produced by accelerated positive ions impacting the negatively biased grids. This effect has been described by Knudsen and Harris.[33] In the extreme retarding portion of sweep A, the current increases with the increasing applied voltage. This current is due to CPE's. The secondary electron current has become comparable to that of the CPE's in sweep B, then dominant in sweep C. The current in the extreme retarding portion of sweep D is due to secondary electrons alone.

The data from orbit #1325 (Figure 2) were taken twelve hours prior to those of #1331 at a time when the southern magnetic pole was near local midnight. Currents observed in the extreme retarding portions of all Mode 2 sweeps are characteristic of secondary electrons only. No CPE fluxes are in evidence. In fact the solar zenith angle along the conjugate orbit (χ_c) was $\geq 116°$ for all values of $L \leq 5.6$

---

33. Knudsen, W.C., and Harris, K.K. (1973) Ion-impact-produced secondary electron emission and its effect on space instrumentation, J. Geophys. Res. 78:1145.
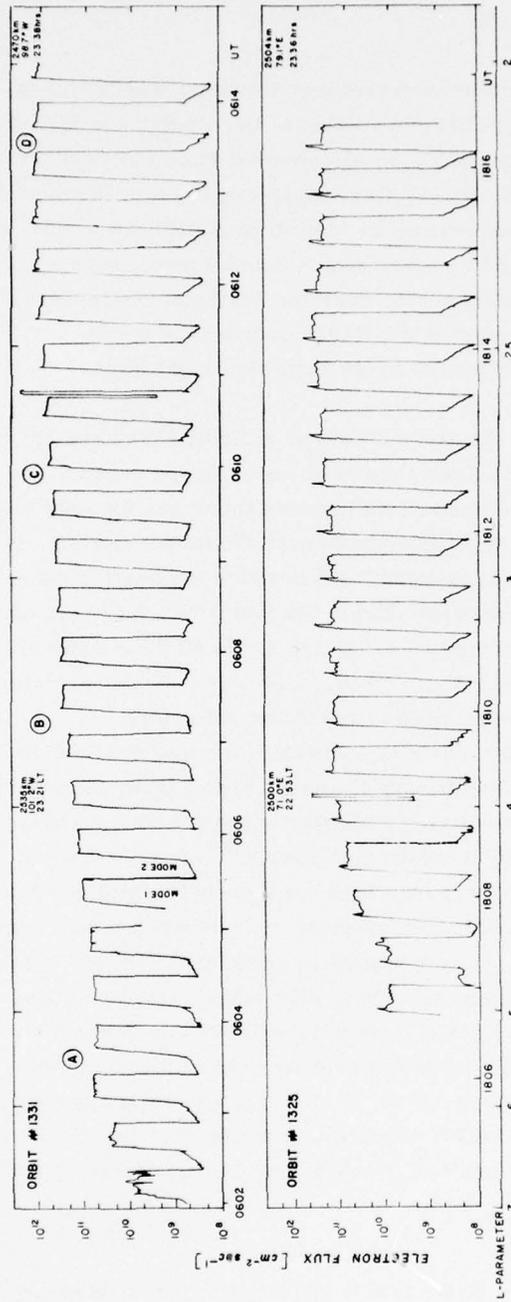
Figure 2. Total Flux Measured by the Electron Sensor During Orbits #1331 and #1325 as a Function of UT and the McIlwain L Parameter. The altitude, longitude, and local time of the satellite at L = 2 and 4 are also given

12

ELECTRON SENSOR SWEEPS
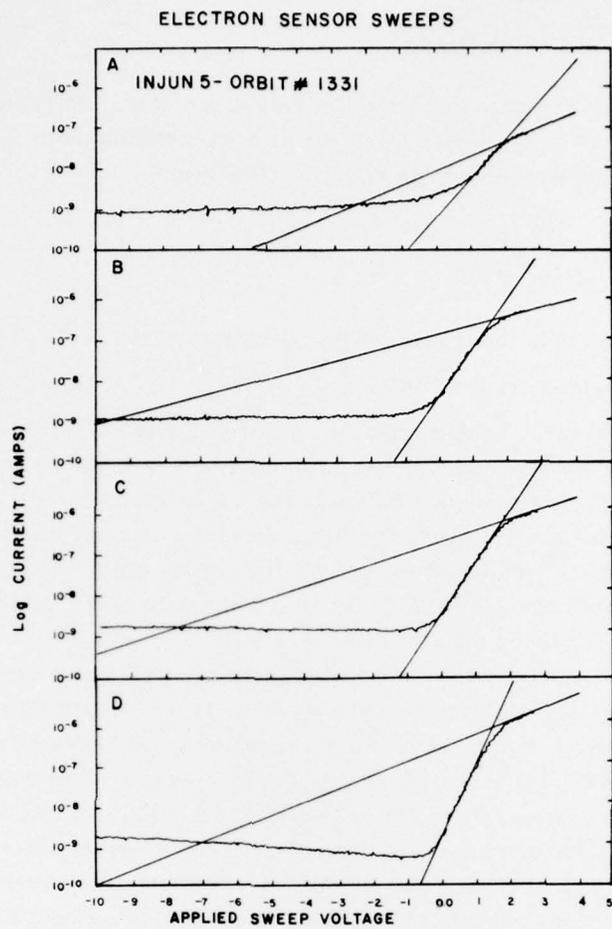
Figure 3.   Mode 2 Sweep at Points Marked A, B,
C, and D of Orbit #1331 in Figure 2

Spectral characteristics of the CPE's can be approximated by an analysis of
the electron sensor sweeps.   Two difficulties are encountered: (1) the Injun 5 SEA
only covers the energy range 0 to 10 eV, and (2) as observed by Injun 5 the CPE's
have been degraded spectrally by collisions with magnetospheric and ionospheric
particles.   Figure 3A shows that in the $-10 \leq V \leq -2V$ range the log vs V charac-
teristic may be well approximated as a straight line from which an effective temp-
erature may be calculated

13

$$T_{CPE} [°K] = \frac{q}{2.3k} \Big/ \left[\frac{d \log I}{d V}\right],$$

where q is the electron charge and k the Boltzmann constant. By projecting the CPE straight line to $V = V_p$, where V_p is the satellite potential with respect to the plasma, it is possible to calculate an effective CPE density

$$N_{CPE} [cm^{-3}] = \frac{I(-V_p)}{\pi R_G^2 \beta q c},$$

where $R_G = 3.18$ cm, β is the transmission coefficient of the grids (0.546) and c the mean thermal velocity of the CPE's $\left[\frac{8k T_{CPE}}{\pi m_e}\right]^{1/2}$. Although the photo-electron spectra measured by Atmospheric Explorer C and E[34] show non-Maxwellian structure for E > 10 eV and a strong low energy component, no significant departures from a Maxwellian distribution in the $2 \leq E \leq 10$ eV range appear in the Injun 5 observations. This result is in agreement with theoretical calculations of Mantas and Bowhill[12] and the observations of Doering et al[34] who noted that spectral fine structure for E < 20 eV found at low altitudes in the sunlit hemisphere was progressively smoothed for altitudes > 250 km.

Because the particle density is low along magnetic field lines intersecting the trough, CPE energy degradation should be minimal at trough latitudes. A Mode 2 current—voltage sweep, typical of trough latitudes at h = 25,000 km from the quiet time orbit #1378 (AE = 14) at Λ = 65.8° is given in Figure 4. The calculated CPE effective density and temperature are 5.3 cm^{-3} and 9.8 eV. On this and all other similar orbits the CPE current characteristic changed to lesser slopes with I (-10 V) remaining almost constant at 9×10^{-9} A as the satellite moved equatorward across the trough. This current corresponds to an omnidirectional flux of CPE's with E > 10 eV of $\sim 3 \times 10^8$ cm^{-2} sec^{-1}. A numerical integration of a recently published spectrum (Figure 5 of Peterson et al)[22] assuming isotropy over the up and down welling hemispheres gives an omnidirectional flux of CPE's with E > 10 eV of 1.4×10^8 cm^{-2} sec^{-1}. Given the different altitudes of the observations, 2500 and 260 km, the agreement is remarkably good. This effect is illustrated in Figure 5 where we have plotted the effective CPE density, temperature as well as I (-10 V) as a function of invariant latitude for orbit #1380. These changes in effective CPE temperature and density indicate that the low energy (E < 10 eV) CPE's lose energy more efficiently than those with higher energy as they move through the ambient plasma along magnetic field lines.[18, 20, 22] The omnidirectional fluxes associated with the CPE observations are between 5×10^8 and 1.1×10^9 cm^{-2} sec^{-1}. The CPE

34. Doering, J.P., Peterson, W.K., Bostrom, C.O., and Potemra, T.A. (1976) High resolution daytime photoelectron energy spectra from AE-E Geophys. Res. Lett. 3:129.

14

heat flux varied between 8.5×10^9 and 1.1×10^{10} eV cm^{-2} sec^{-1}. The particle fluxes are consistent with those reported by Heikkila,[19] but a factor of three higher than those reported by Maier and Rao.[17]

INVARIANT LATITUDE = 65.8°

ALTITUDE	2533 km
LOCAL TIME	22:50
< A E >	14

INJUN 5 ORBIT #1378
11-30-68

T_e = 7737 °K
N_e = 165 cm^{-3}
T_{CPE} = 9.8 eV
N_{CPE} = 5.3 cm^{-3}
V_s = -2.2 VOLTS

ELECTRON CURRENT [AMPS]

APPLIED SWEEP VOLTAGE [VOLTS]
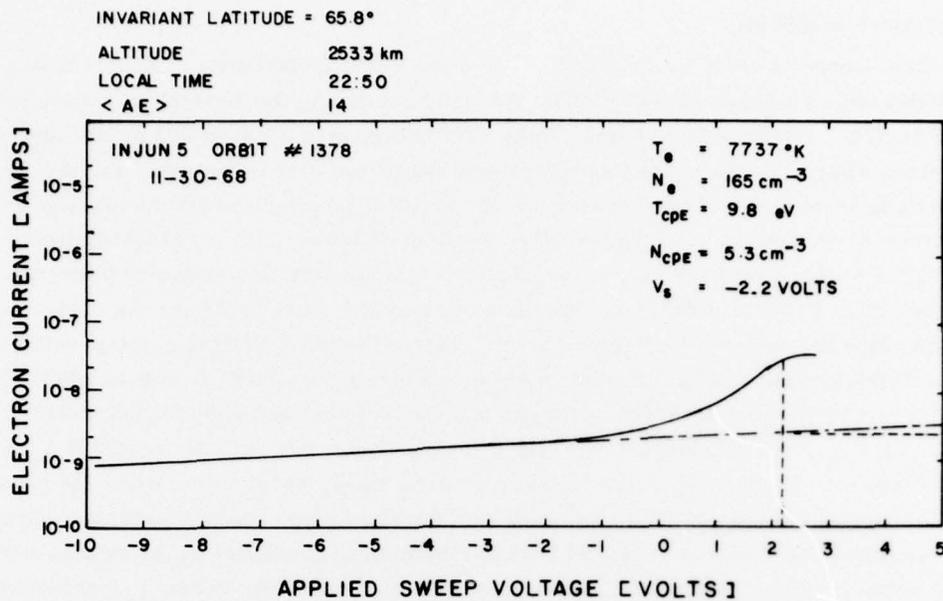
Figure 4. A Typical Plasma Trough Observation of Conjugate Photoelectrons in the Quiet Time Plasma Trough. The CPE temperature and density may be calculated knowing the slope of the characteristic in the extreme retarding portion of the sweep and the vehicle potential with respect to the plasma

Injun 5 Orbit #1380

$I(V=10)$ (amps)

× T_{CPE} (eV)
⊙ N_{CPE} (cm-3)

CPE Temperature and Density

Invariant Latitude
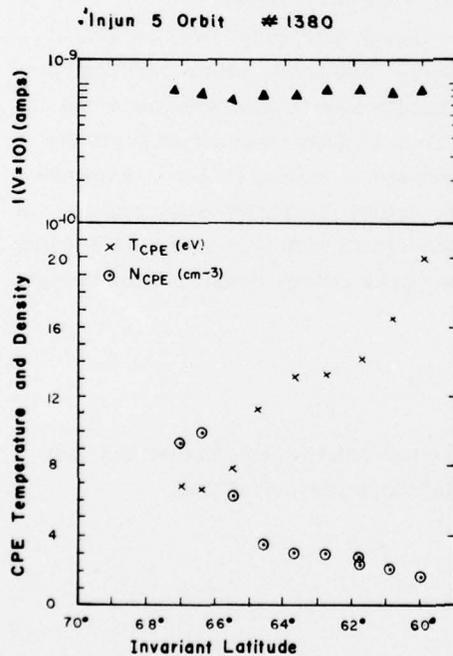
Figure 5. The Effective CPE Temperature (χ) and Density (⊙) Observed During the Injun 5 Orbit #1380 as a Function of Invariant Latitude (lower portion). The current measured at V = -10 V on the Mode 2 sweeps as a function of invariant latitude (Λ) are given in the upper portion of the figure

15

3.2 Results Near 2500 km

Data were collected on 25 orbits while Injun 5 was in darkness at subauroral latitudes and at altitudes between 2200 and 2500 km during the November-December 1968 period. Twenty-two of these orbits were distributed between 60° W and 120° W longitude where the conjugate ionosphere was sunlit for part of the orbit and the remaining three orbits were between 70° E and 90° E longitude where the conjugate ionosphere was totally in darkness. The heating effects of CPE's are illustrated in Figure 6 where we have plotted the electron temperature and densities observed during orbits #1325 and #1331 as functions of invariant latitude (Λ) and the solar zenith angle (χ_c) along the conjugate orbit. Within the trough electron temperatures are relatively high in both instances. Equatorward of the trough T_e fell to 2300 °K ($\chi_c > 118°$) in the case of #1325, whereas it remained between 4500 °K and 4000 °K to $\Lambda = 51°$ ($\chi_c = 105°$) during #1331. As χ_c passed from 105° to 120° on #1331 T_e decreased to a value comparable to that observed during #1325 at the same latitude.

All orbits between 2200 km and 2500 km exhibited high, sharply peaked electron temperature distributions at trough latitudes with steep gradients at the equatorward edge of the trough. In the three cases with shadowed conjugate orbits T_e decreased to 2300 °K at mid-latitudes. The cases with sunlit conjugate orbits had an electron temperature plateau with $3800 \leq T_e \leq 4500$ °K which decreased to ~2300 °K as the conjugate ionosphere passed into darkness. This indicates that near 2500 km the CPE's raised the ionospheric electron temperature between 1500 and 2200 °K at latitudes between the equatorward edge of the trough and conjugate sunset.

Although CPE's certainly contribute to the trough electrons' heat budget, it appears that another source must also be invoked. The cases with a darkened conjugate ionosphere showed significant electron temperature enhancements in the plasma trough. A likely candidate might appear to be heat transported from the auroral zone to the trough. However the highest electron temperatures were observed during orbits #1378 and #1380 when the auroral electrojet index was 14. As expected, the position of the trough moved equatorward with increasing AE leading to higher trough densities. It was found that the peak energy density in the trough did correlate with AE

$$n_e k T_e \ [eV/cm^{-3}] = 73.2 + 0.62 \ AE$$

with a correlation coefficient of 0.70. We have not determined whether the heat source lies in the quiet time ring current or diffuse aurora electrons.

16
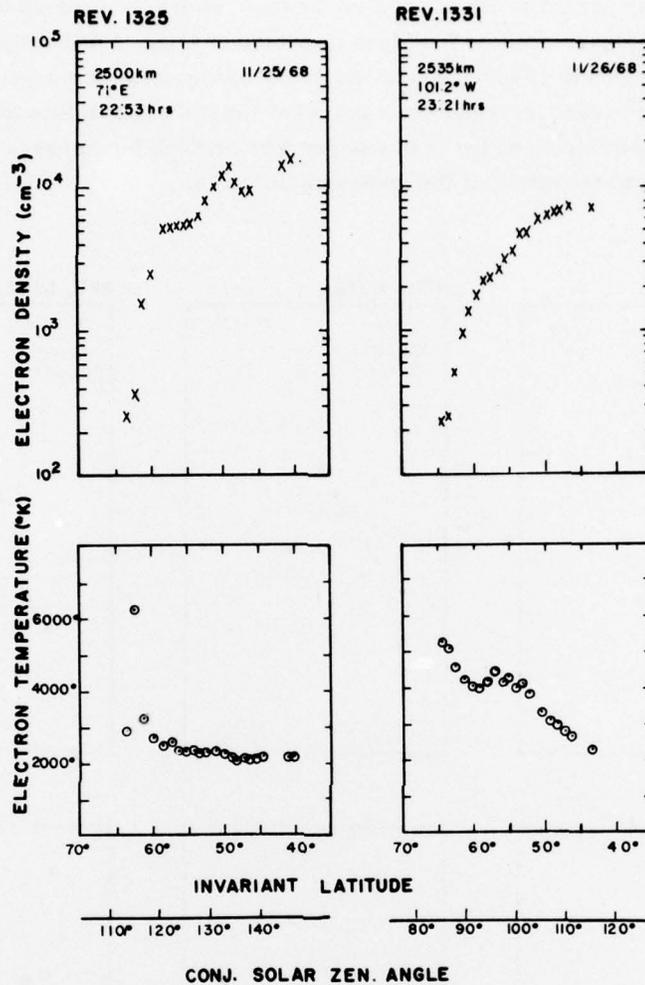
Figure 6.   The Electron Densities and Temperature
Observed During Orbits #1325 and #1331 as Functions
of Invariant Latitude and the Conjugate Solar Zenith
Angle.   The altitude, longitude, and local time of the
satellite at Λ = 60° are given

3.3   Results From Below 1400 km

Data were taken on twenty-eight Injun 5 orbits between 9 and 25 January 1970
in the altitude range $1400 \geq h \geq 850$ km, at this time the satellite was descending
toward perigee near the equator.   Seven of the orbits were from the 50° to 90° E
longitude sector, seventeen from the 60° to 130° W longitude sector with the re-
mainder scattered between 20° E and 20° W.   A high degree of variability appears

17

in data from this period as illustrated in Figure 7 where we have plotted electron densities and temperatures as functions of invariant latitude and conjugate solar zenith angle for orbits #6330, #6332, and #6337 on the magnetically quiet day 11 January. The altitude, longitude, and local time of the satellite at $\Lambda = 60°$ are given. Altitude differences between eastern and western hemisphere orbits at $\Lambda = 60°$ are due to the offset of the geomagnetic poles.
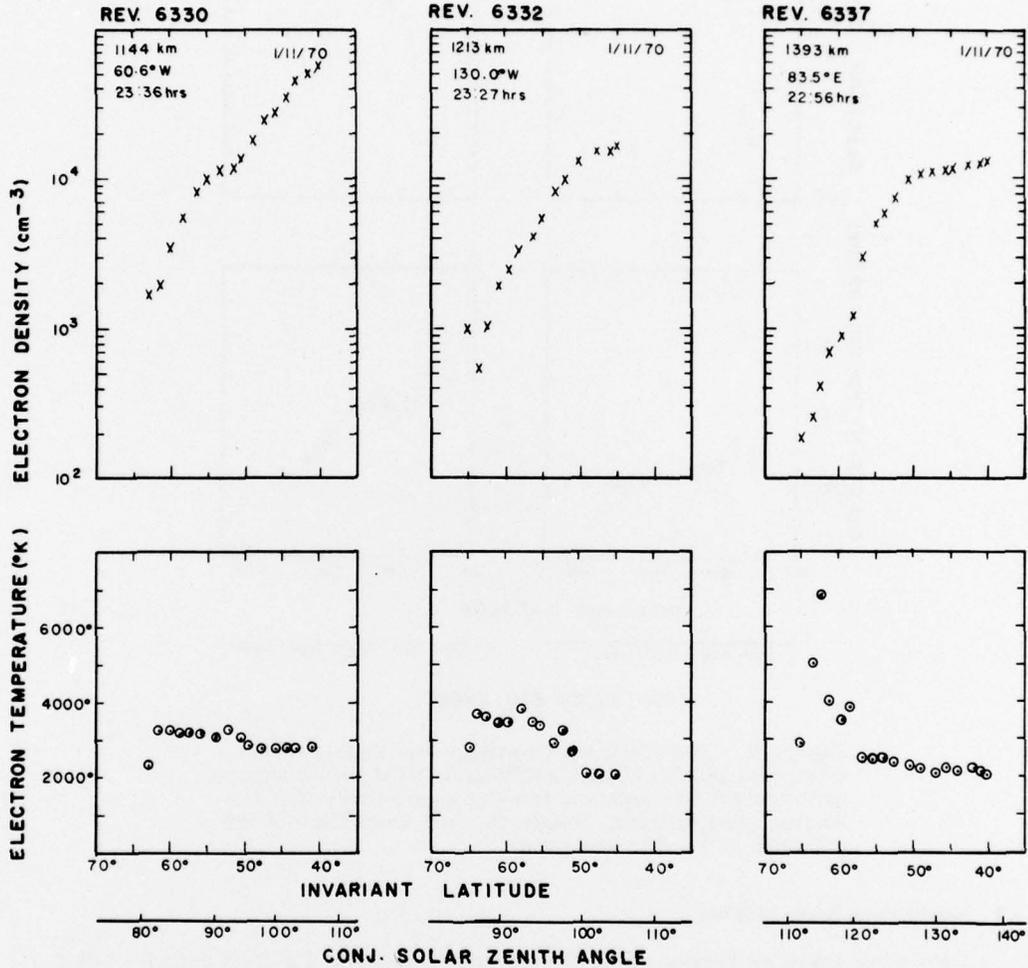
Figure 7. The Electron Densities and Temperatures Observed During Orbits #6330, #6332, and #6337, on the Magnetically Quiet Day 11 January 1970, as Functions of Invariant Latitude and the Conjugate Solar Zenith Angle. The altitude, longitude, and local time of the satellite at $\Lambda = 60°$ are given

18

Along orbit #6330 the electron temperature was nearly constant at ~3200 °K from the trough to $\Lambda = 50°$ ($\chi_c \simeq 95°$) where it decreased to ~2800°. This temperature maintained to $\Lambda = 30°$ (data not shown) where T_e further decreased to ~2000 °K. The electron temperature remained near this level until the satellite passed into sunlight at 46° S, 48° W ($\Lambda = 38°$), and at an altitude of 780 km. The temperatures observed during #6332 remained near 3700 °K from the trough to $\chi_c \simeq 95°$ where T_e decreased to ~2100 °K. The temperature distribution observed during #6337 resembled that observed during #1325 (Figure 6). A highly peaked temperature in the trough decreased to values between 2000 °K to 2500 °K at mid-latitudes where $\chi_c > 120°$.

In many respects data from the three orbits given in Figure 7 are representative of the entire January 1970 data set. Except in four cases where relatively deep troughs were found, in western hemisphere orbits between 1200 and 850 km, no pronounced temperature maxima were observed in the trough. In six of the seventeen orbits between 60° W and 130° W the maximum electron temperatures were found equatorward of the trough. At mid-latitudes, as in the case of #6330, all orbits between 60° W and 100° W maintained electron temperatures in excess of 2500 °K to $\Lambda = 30°$, well equatorward of nominal conjugate sunset. This is an unexplained feature of the observations. All orbits between 110° W and 130° W, were characterized by electron temperatures of ~2100 °K for $\chi_c > 100°$, as illustrated by #6332 (Figure 7).

All of the orbits over the eastern hemisphere were characterized by maximum temperatures at trough latitudes and electron temperatures between 2000 °K and 2500 °K equatorward of the trough. It was noted however, that as the satellite descended to 1100 ± 50 km over the eastern hemisphere the maximum electron temperature in the trough decreased to ~3500 °K. This value is comparable to the trough temperatures observed on orbits #6330 and #6332 at approximately the same altitudes.

4. DISCUSSION

In the previous section we presented the longitudinal and latitudinal electron temperature distributions observed in the nightside ionosphere near the 1968 and 1969 winter solstices. Here we assume that the measurements taken by means of Injun 5 represent a random sampling of the typical, quiet-time, winter topside ionosphere. This assumption allows us to consider, in a statistical sense, the altitude dependence of the electron temperatures and to draw interference relating to physical processes in the ionosphere. Effective spectral characteristics of CPE's are studied as functions of altitude at trough latitudes. Due to the obscuring

19

effects of instrument generated secondary electrons this cannot be done equatorward of the trough. On the basis of the results presented in the last section the observations are divided into those of the trough and those of the region equatorward of the trough.

4.1 Trough Latitude

At trough latitudes, near satellite apogee, the electron temperatures were highly peaked. The result is in substantial agreement with results from ISIS I at 3000 km.[35] The electron temperature peak was not a consistent feature at altitudes below 1200 km. The maximum electron temperatures and corresponding energy density observed in the trough on 57 Injun 5 orbits are plotted as functions of altitude in Figure 8. Data from seven orbits during December 1969 at altitudes between 1500 and 2200 km were included. Three orbits previously considered were excluded here owing to data gaps in the trough. In cases of no clear maximum temperature in the trough, the temperature at minimum electron density was chosen to represent the orbit. These orbits have $T_{max} < 3000\,°K$.

A linear regression analysis performed on the electron temperatures vs altitude (Figure 8) gave

$$T_e\ (°K) = 2.03h + 1420 \tag{1}$$
$$850 \leq h \leq 2500 \text{ km .}$$

A similar least squares analysis of the electron energy density data gave

$$\ln \epsilon \left(\frac{eV}{cm^3} \right) = 10.561 - 0.00385h \tag{2}$$
$$850 \leq h \leq 1500 \text{ km}$$

93 percent of the data points lie within a factor of two of this regression line. The exceptional points were measured during times of substorm activity as evidenced by AE indices of 338 and 204. The data taken between 850 and 1500 km indicates a situation analogous to diffusive equilibrium with a scale height of 260 km. Above 1500 km electron energy densities were between 50 and 200 eV/cm^3 and showed no systematic variation with altitude.

---

35. Brace, L.H., and Theis, R.F. (1974) The behavior of the plasmapause at mid-latitudes: Isis 1 Langmuir probe measurements, J. Geophys. Res. 79:1871.
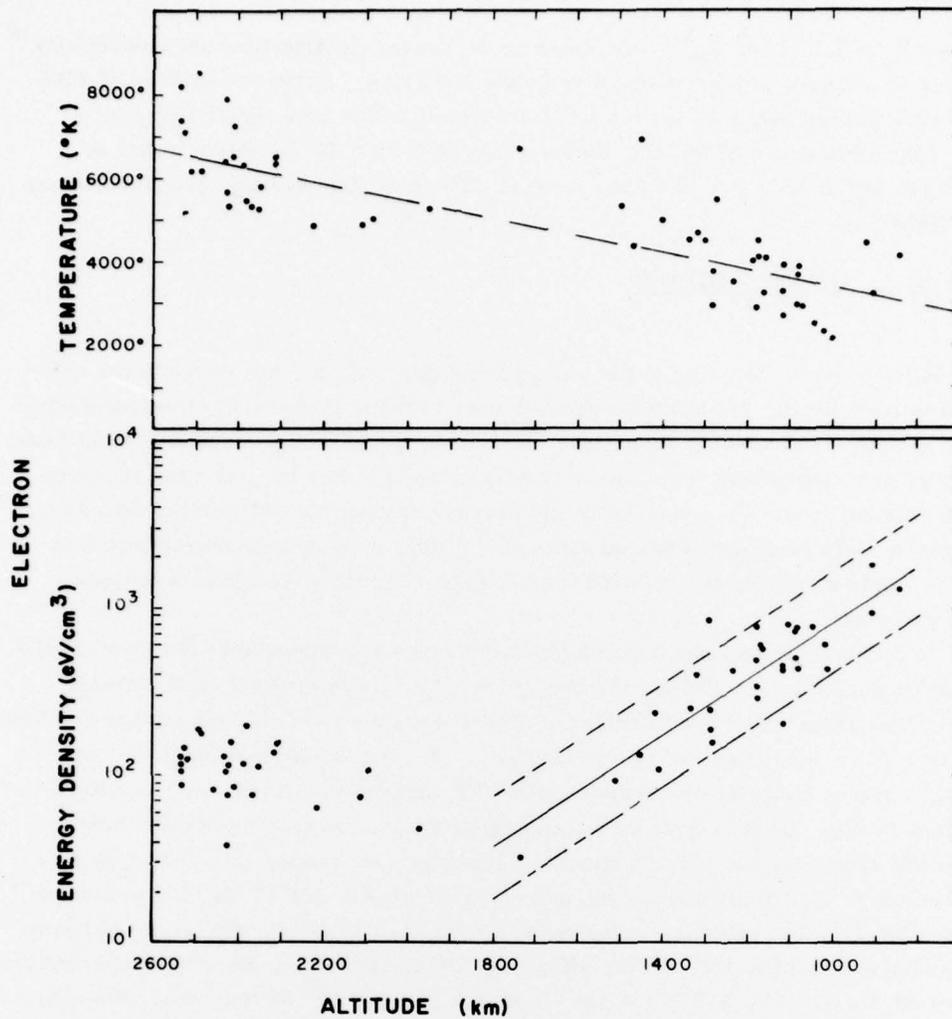
Figure 8. Maximum Electron Temperatures and Corresponding Energy Densities as a Function of Altitude Observed on 57 Injun 5 Orbits in the Trough. The dashed line on the upper plot results from a linear regression analysis of the data points. The regression line on the lower plot was calculated for points below 1500 km. The dashed lines are meant to show that 93 percent of these data lie within a factor of two of the regression line

The results summarized in Figure 8 and Eqs. (1) and (2) cannot be interpreted simply. For a fully ionized plasma the electron heat flux along the magnetic field lines is

$$Q = -K_e \frac{dT_e}{ds} . \tag{3}$$

21

Where $K_e = 7.7 \times 10^5 \, T_e^{5/2}$ (eV/cm-sec-deg) is the electron thermal conductivity[36] and ds is a length element along a magnetic field line. Between altitudes of 2500 and 1000 km the length of the $\Lambda = 63°$ field line is ~1620 km. Since $(dT_e/ds) \simeq (dT_e/dh)(dh/ds) = 1.88$ °K/km, the heat flux is 4.91×10^{10} (eV/cm^3-sec) at 2500 km and 1.02×10^{10} (eV/cm^2-sec) at 1000 km. The average heat input along the field line

$$\frac{dQ}{ds} \approx \frac{Q(2500) - Q(1000)}{\Delta s}$$

is ~240 (eV/cm^3-sec). Since the energy input per cm^3 in 1 sec exceeds the electron energy density for altitudes greater than 1300 km (Figure 8), processes other than simple electron-heat conduction must occur along trough connected field lines. Energy can be removed from the ambient electrons either by: (1) heat exchange with ambient ions, (2) cross-field line heat conduction, or (3) plasma flow along magnetic field lines out of the ionosphere.[37] With present instrumentation it is not possible to assess the relative importance of the three electron heat-loss mechanisms.

In Section 3 it was noted that high electron temperatures were observed in the trough independent of whether the conjugate orbit was in sunlight or darkness. From this observation it was inferred CPE's were not the only heat source available to the topside ionosphere at trough latitudes. Further confirmation of the conjecture can be obtained by examining the CPE input in the North American longitudinal sector. This is done by examining CPE spectral characteristics near satellite apogee and at lower altitudes. In orbits near apogee (h = 2528 ± 16 km) the effective CPE temperature and density were 10.4 ± 2.6 eV and 5.2 ± 1.9 cm^{-3} respectively. The effective heat flux was $9.4 \pm 1.0 \times 10^9$ eV/cm^2 sec. At lower altitudes (h = 1114 ± 120 km) the effective CPE temperature, density, and heat flux were 13.1 ± 3.8 eV, 3.6 ± 1.3 cm^{-3} and $9.2 \pm 1.5 \times 10^9$ eV/cm^2 sec. We also calculated the CPE heat loss in the 1000 ≤ h ≤ 2500 km altitude range using the formula derived by Swartz et al.[38] Ambient electron conditions were approximated using data from Figure 8. The calculations show that CPE's with E > 2 eV lose less than 3 percent of their energy in this altitude range. From these and above given calculations we conclude that at trough latitudes: (1) heat deposited by conduction from above is much greater than the deposited locally by CPE's, and (2) the bulk of the CPE heat loss occurs at altitudes less than 1000 km.

36. Spitzer, L. (1967) Physics of Fully Ionized Gases, Interscience, New York.

37. Banks, P. M., and Doupnik, J. R. (1974) Thermal proton flow in the plasmasphere: the moring sector, Planet. Space Sci. 22:79.

38. Swartz, W. E., Nisbet, J. S., and Green, W. E. S. (1971) Analytic expression for the energy transfer rate from photoelectrons to thermal electrons, J. Geophys. Res. 76:8421.

4.2 Equatorward of the Trough

Equatorward of the trough the electron temperature distributions observed over the North American and the Asian longitudinal sectors were quite different. In the Asian sector midlatitude electron temperatures were between 2000 °K and 2500 °K over the $1200 \leq h \leq 2500$ km altitude range. That is, where the conjugate ionosphere is in darkness the ionosphere is close to isothermal. At longitudes and latitudes where the conjugate ionosphere was sunlit $T_e \simeq 4000$ °K at 2500 km and $T_e \simeq 3000$ °K at 1000 km. The length of the $\Lambda = 55°$ field line is ~1650 km between 2500 and 1000 km altitude. Thus, the electron temperature gradient along this magnetic field line is 0.61 °K/km. From Eq. (6) we calculate a heat flux of 4.72×10^9 eV/cm^2-sec at 2500 km and 2.27×10^9 eV/cm^2-sec at 1000 km, the average heat input along the field line is 15 eV/cm^3-sec.

CPE fluxes at sub-trough latitudes are partially obscured by instrumental secondary electron fluxes at 2500 km and totally obscured at 1000 km. Thus it is impossible to measure directly the amount of thermal energy deposited locally by CPE's using Injun 5 instrumentation. The latitudinal distribution of effective CPE densities and temperatures (Figure 5) and the calculations of LeJeune and Wormser[13] indicate that a significant portion of the CPE energy loss occurs at altitudes > 2500 km in the protonosphere. The energy deposited at these high altitudes would be conducted down magnetic field lines into the topside ionosphere. The higher energy component of the CPE spectrum (> 10 eV) penetrates to the lower portion of the F region[22] before losing energy via ionization[15] and heating[14] processes.

5. SUMMARY AND CONCLUSIONS

In this report we have examined the thermal and hyperthermal fluxes of electrons measured with a gridded, spherical electrostatic analyzer aboard Injun 5. The measurements were taken in the northern hemisphere near the times of the 1968 and 1969 winter solstices. At these times the satellite was near local midnight in the altitude range $850 \leq h \leq 2550$ km. Electron temperatures were examined as functions of latitude and longitude to determine the heating effects of conjugate photoelectrons on the topside ionosphere. This was accomplished by using the fact that due to the offset between the geographic and geomagnetic poles the CPE's have access to the Atlantic Ocean and North American but not to the Asian longitude sector.

At trough latitudes the CPE's had effective densities and temperatures of ~5 cm^{-3} and ~9 eV. Equatorward of the trough the effective density decreased and the effective temperature increased indicating that a significant fraction of the low energy component of the CPE spectrum was lost while passing through the protonosphere.

23

At altitudes near 2500 km ambient electron temperatures had maximum values in the region of the trough. Equatorward of the trough the electron temperature was ~2300 °K over the Atlantic Ocean-North American longitude sector. Over the Asian longitude sector, the electron temperature was ~2300 °K for sub-trough latitudes. At altitudes near 1000 km the electron temperature peak in the trough was not a consistent feature of the data. Equatorward of the trough the electron temperatures were ~3000 °K to the latitude of conjugate sunset. The temperature drop at conjugate sunset over the Atlantic Ocean and North America was not as great as it was over the eastern Pacific Ocean or the Asian longitude sectors.

On the basis of these data it is concluded that:

(1) Elevated electron temperatures observed in the trough between 1000 and 2500 km are independent of longitude and are produced by sources other than CPE's,

(2) Electron temperature and energy density distributions in the trough are not consistent with a simple electron heat conduction model for energy transport. Electron energy loss mechanisms must also be operative in the $1000 \leq h \leq 2500$ km altitude range,

(3) Most of the energy deposited by CPE's in the trough occurs at altitudes less than 1000 km,

(4) Equatorward of the trough a significant fraction of the CPE energy is deposited at altitudes > 2500 km. This energy is then conducted down the magnetic field lines into the topside ionosphere. The higher energy component of the CPE spectrum is lost at altitudes much lower than 1000 km.

References

1. Hanson, W. B. (1963) Electron temperature in the upper atmosphere, Space Research 3:282-302.

2. Cicerone, R. J., Schwartz, W. E., Stolarski, R. S., Nagy, H. F., and Nisbet, J. S. (1973) Thermalization and transport of photoelectron: a comparison of theoretical approaches, J. Geophys. Res. 78:6709-6728.

3. Swartz, W. E. (1976) Thermalization and transport of photoelectrons: a comparison of theoretical approaches 2. Transport details for isotropic scattering, J. Geophys. Res. 81:183-192.

4. Nisbet, J. S. (1968) Photoelectron escape from the ionosphere, J. Atm. Terr. Phys. 30:1257-1278.

5. Swartz, W. E. (1972) Electron Production Recombination and Heating in the F Region of the Ionosphere, Sci. Rep. 381, Ionosphere Res. Lab., Pa. State University, University Park.

6. Nagy, A. F., and Banks, P. M. (1970) Photoelectron fluxes in the ionosphere, J. Geophys. Res. 75:6260-6270.

7. Banks, P. M., and Nagy, A. F. (1970) Concerning the influence of elastic scattering upon photoelectron transport and escape, J. Geophys. Res. 75:1902-1910.

8. Stolarski, R. S. (1972) Analytic approach to photoelectron transport, J. Geophys. Res. 77:2862-2870.

9. Cicerone, R. J., and Bowhill, S. A. (1970) Photoelectron escape fluxes obtained by a Monte Carlo technique, Radio Science, 5:49-53.

10. Cicerone, R. J., and Bowhill, S. A. (1971) Photoelectron fluxes in the ionosphere computed by a Monte Carlo method, J. Geophys. Res. 76:8299-8317.

11. Mantas, G. P., and Bowhill, S. A. (1975) Calculated photoelectron pitch angle and energy spectra, Planet. Sp. Sci. 23:355.

12. Mantas, G. P. (1975) Theory of photoelectron thermalization and transport in the ionosphere, Planet. Sp. Sci. 23:337.

25

13. Lejuene, G., and Wormser, F. (1976) Diffusion of photoelectrons along a field line inside the plasmasphere, J. Geophys. Res. 81:2900.

14. Mantas, G. P., and Walker, J. C. G. (1976) The penetration of soft electrons into the ionosphere, Planet. Sp. Sci. 24:409.

15. Shawhan, S. D., Block, L. P., and Falthammer, C. G. (1970) Conjugate photo-electron impact ionization, J. Atm. Terr. Phys. 32:1885.

16. Rao, B. C. N., and Donley, J. L. (1969) Photoelectron flux in the topside ionos-sphere measured by retarding potential analyzers, J. Geophys. Res. 74:1715.

17. Maier, E. J., and Rao, B. C. N. (1970) Observations of the suprathermal electron flux and the electron temperature at high latitudes, J. Geophys. Res. 75:7168-7174.

18. Rao, B. C. N., and Maier, E. J. R. (1970) Photoelectron flux and protonospheric heating during the conjugate point sunrise, J. Geophys. Res. 75:816.

19. Heikkila, W. J. (1970) Photoelectron escape flux observations at mid-latitudes, J. Geophys. Res. 75:4877-4879.

20. Galperin, Y. I., Dymek, M., Kutiev, I., Mulyarchik, T. M., Serafimov, K. B., Shuiskaya, F. K., and Wernik, S. (1973) Spectra of ionospheric photoelectrons and their transport from conjugate ionosphere, Ann. Geophys. 29:117.

21. Doering, J. P., Peterson, W. K., Bostrom, C. O., and Armstrong, J. C. (1975) Measurement of low energy electrons in the day airglow day side auroral zone Atmosphere Explorer C, J. Geophys. Res. 80:3934.

22. Peterson, W. K., Doering, J. P., Potemera, T. A., McEntire, R. W., and Bostrom, C. O. (1977) Geophys. Res. Lett. 4:109.

23. Barbier, D. (1959) Recherches sur la raie 6300 de la luminescence atmos-pherique nocturne, Ann. Geophs. 15:179-186.

24. Carlson, H. C. (1974) Survey of satellite and ground based measurements of photoelectron excited emissions, Ann. Geophys. 30:59.

25. Carlson, H. C. (1966) Ionospheric heating by magnetic conjugate-point photo-electrons, J. Geophys. Res. 71:195.

26. Evans, J. V., and Gastman, I. J. (1970) Detection of conjugate photoelectrons at Millstone Hill, J. Geophys. Res. 75:807.

27. Evans, J. V. (1968) Sunrise behavior of the F layer at midlatitudes, J. Geophys. Res. 73:3489.

28. Nagy, A. F., Winningham, J. D., and Banks, P. A. (1973) The effect of con-jugate photoelectron impact ionization on the pre-dawn ionosphere, J. Atm. Terr. Phys. 35:2289.

29. Burke, W. J., Donatelli, D. E., and Sagalyn, R. C. (1978) Injun 5 observations of low energy plasma in the high latitude topside ionosphere, (to be published J. Geophys. Res.).

30. Mott-Smith, H. M., and Langmuir, I. (1926) The theory of collectors in gaseous discharges, Phys. Rev. 28:727-763.

31. Rao, L. V. D., Burke, W. J., Kanal, M., and Sagalyn, R. C. (1978) Injun 5 low energy plasma observations during a major magnetic storm, (to be published J. Geophys. Res.).

26

32. Gustafson, G. (1970) A revised corrected geomagnetic coordinate system, Arkiv for Geofysik 5:595-617.

33. Knudsen, W.C., and Harris, K.K. (1973) Ion-impact-produced secondary electron emission and its effect on space instrumentation, J. Geophys. Res. 78:1145.

34. Doering, J.P., Peterson, W.K., Bostrom, C.O., and Potemra, T.A. (1976) High resolution daytime photoelectron energy spectra from AE-E, Geophys. Res. Lett. 3:129.

35. Brace, L.H., and Theis, R.F. (1974) The behavior of the plasmapause at mid-latitudes: Isis 1 Langmuir probe measurements, J. Geophys. Res. 79:1871.

36. Spitzer, L. (1967) Physics of Fully Ionized Gases, Interscience, New York.

37. Banks, P.M., and Doupnik, J.R. (1974) Thermal proton flow in the plasmasphere: the moring sector, Planet. Space Sci. 22:79.

38. Swartz, W.E., Nisbet, J.S., and Green, W.E.S. (1971) Analytic expression for the energy transfer rate from photoelectrons to thermal electrons, J. Geophys. Res. 76:8421.